Applied Biochemistry and Biotechnology (2020) 190:634–644
https://doi.org/10.1007/s12010-019-03101-2

Studies on the Neuroprotection of Osthole on Glutamate-Induced Apoptotic Cells and an Alzheimer's Disease Mouse Model via Modulation Oxidative Stress

Qiubo Chu[1,2] · Yanfeng Zhu[2] · Tianjiao Cao[2] · Yi Zhang[2] · Zecheng Chang[3] · Yan Liu[2] · Jiahui Lu[2] · Yizhi Zhang[1]

Received: 4 June 2019 / Accepted: 18 July 2019 /
Published online: 13 August 2019

Abstract
In the present study, the neuroprotection of osthole (OST) was confirmed. In L-glutamic acid (L-Glu)-damaged HT22 cells, a 3-h pre-incubation with OST-enhanced cell viability suppressed the apoptosis rate; inhibited the activities of caspase-3, caspase-8, and caspase-9; reduced the over-accumulation of intracellular reactive oxygen species; restored the dissipated mitochondrial membrane potential; and regulated the expression levels of B cell lymphoma-2 (Bcl-2), Bax, cleaved poly (ADP-ribose) polymerase (PARP), NF-E2p45-related factor 2 (Nrf2), and its downstream proteins. In amyloid precursor protein/presenilin 1 (APP/PS1) transgenic mice, an 8-week OST administration improved the pathological behaviors related to memory and cognition, and reduced the expression levels of 4-hydroxynonenal, the deposition of β-amyloid peptides and neuronal fiber tangles formed by the high phosphor-Tau in the brain. OST enhanced the expression levels of Nrf2 and its downstream proteins including superoxide dismutase-1 (SOD-1) and heme oxygenase-1 (HO-1). The present data confirmed the protection of OST against AD-like symptoms via modulating oxidative stress, especially Nrf2 signaling.

Keywords Osthole · Alzheimer's disease · Apoptosis · Oxidative stress · Nrf2

Introduction

As one of the high-profile of dementia, Alzheimer's disease (AD) is known as the cognitive dysfunction due to the damage on neurons [1]. According to the previous research, the over-exited amyloid beta (Aβ) deposit and the over-formatted neuronal fiber tangles by the hyper-levels of phosphorylated (P)-Tau show direct effect on disruption of oxidative balance and

✉ Yizhi Zhang
yzzhang@jlu.edu.cn

Extended author information available on the last page of the article

damage on neurons [2, 3]. The occurrence of oxidative stress has been noted in the development of AD in patients, and especially indicated by the remarkable accumulation of reactive oxygen species (ROS), which promotes Aβ aggregation due to the damage of mitochondria and nucleic acid [1]. Furthermore, the high concentration of glutamate associated with ROS excessive accumulation and mitochondrial dysfunction directly causes brain excitement and neuron damage [4]. As an important protein within cellular redox homeostasis, NF-E2p45-related factor 2 (Nrf2) helps to modulate the mitochondria function, further regulating the levels of Aβ in mice with AD-like behaviors [5].

The prevention and therapy of AD is still an enormous challenge globally, and natural compounds have been an underutilized potential source for screening candidates on AD treatment [6]. Osthole (OST), a natural coumarin extracted from *Cnidium monnieri* fruits, has various pharmacological activities including anti-inflammation, anti-tumor, anti-arrhythmia, lowering blood pressure, and enhancing immunity [7]. Accordingly, it is reported that OST possesses anti-oxidative and anti-apoptotic properties [8]. However, the neuroprotection of OST against AD-like behaviors performing in cells and gene transgenic mice, as well as the underlying mechanisms, has not been well studied.

In the present study, the neuroprotection of OST was successfully confirmed in L-Glu caused apoptotic HT22 cells and the amyloid precursor protein/presenilin 1 (APP/PS1) transgenic mice, which may be related to its regulation on Nrf2-mediated metachronal apoptosis. The present study provides the evidences for further investigating the possibility of OST as a candidate for AD therapy.

Method and Materials

Cell Culture

HT22 cells, the mouse hippocampal neurons, were obtained from the Cell Bank of Chinese Academy of Science (Shanghai, China). HT22 cells were cultured in the atmosphere of 5%/95% CO_2/air at 37 °C using the Dulbecco's modified Eagle's medium (DMEM) which contains 10% fetal bovine serum, 100 U/mL of penicillin, and 100 μg/mL streptomycin. All reagents were obtained from Beijing Solarbio Science & Technology Co., Ltd. (Beijing, China).

The Detection of Cell Viability

The seeded HT22 cells in 96-well plates underwent 3-h pre-incubation with OST (CAS no. 484-12-8) (Sigma-Aldrich, Burlington, MA, USA) at doses of 20 and 40 μM prior to 24-h co-incubation with L-Glu (25 mM) (Invitrogen, Carlsbad, CA, USA), and then the cell viability is detected similar as the previous study using 3-(4,5-dimethylthiazol-2-yl)-2,5-diphenyltetrazolium bromide (MTT) (Invitrogen, Carlsbad, CA, USA) method [9].

The Detection of Cell Apoptosis, the Activities of Caspase-3, Caspase-8, and Caspase-9, the Levels of Mitochondrial Membrane Potential (MMP) and ROS

The seeded HT22 cells in 6-well plates underwent the 3-h pre-incubation with OST at doses of 20 and 40 μM prior to 24-h co-incubation with L-Glu (25 mM). The treated cells were

collected and stained with propidium iodide and Annexin V (Invitrogen, Carlsbad, CA, USA) for 15 min at 25 °C in the darkness, and their apoptotic rate was analyzed using the Muse™ Cell Analyzer flow cytometer (EMD Millipore, USA).

The treated cells were collected, lysed, and analyzed the activities of caspase-3 (APT129), caspase-8 (APT131), and caspase-9 (APT139) (EMD Millipore, USA) using the commercially available kits according to the manufacturer's protocols.

For MMP detection, treated cells were exposed to 2 μM of 5,5′,6,6′-tetrachloro-1,1′,3,3′-tetraethyl-imidacarbocyanine iodide stain (JC-1) (T3168, Invitrogen, Carlsbad, CA, USA) for 15 min at 25 °C in the darkness. The changes of the fluorescence intensities of the cells was detected by a fluorescence microscope (IX73; Olympus, Japan).

For ROS detection, treated cells were exposed to 10 μM of 2′-7′-dichlorodihydrofluorescein diacetate (DCFH-DA) (D6470, Beijing Solarbio Science & Technology Co., Ltd. Beijing, China) for 15 min at 25 °C in darkness. The changes of the fluorescence intensities of the cells was detected by a fluorescence microscope (IX73; Olympus, Japan).

ImageJ software version 1.46 (National Institutes of Health, USA) was applied to quantify the fluorescence intensities.

The Experimental Process Performed in APP/PS1 Mice

The experiments on APP/PS1 mice were approved by the Animal Ethics Committee of the Second Hospital of Jilin University (20171201). Thirty-six 8-month-old B6C3-Tg APP/PS1 male mice were randomly divided into three groups and gavaged with double-distilled (D.D.) water serving as model group ($n = 12$), and OST at doses of 15 and 30 mg/kg ($n = 12$/group) once daily for 56 days. Twelve 8-month-old wild-type male mice were gavaged with D.D. water serving as control group ($n = 12$) once daily for 56 days. All mice (SCXK (Su) 2015-0001) were purchased from Nanjing Biomedical Research Institute of Nanjing University, Nanjing, China, and housed in an environment with a temperature of 23 ± 1 °C and humidity of 40–60% with a 12-h light/dark cycle. Food and water were provided ad libitum.

Behavioral Tests

Morris Water Maze Test

Similar as previous study [9], Morris water maze (MWM) test was applied to analyze the learning and memory abilities of mice in the present study on the 57th day after a 7-day training for all mice.

Open-field Experiment Test

Similar as previous study [9], the open-field test was applied to analyze the autonomous behaviors of mice on the 58th day.

Immunohistochemical Examination

After the behavioral tests, all mice were euthanized, and then the whole brains were collected. One part of brain tissues was used for the immunohistochemical examination. According to the

previous protocol [10], after deparaffinization and hydration, the sections of brains (5 μm) were incubated with 3% hydrogen peroxide for 10 min for antigen retrieval. Following with the blocking with 10% goat serum (Beijing Solarbio Science & Technology Co., Ltd., Beijing, China), the sections were incubated with 4-hydroxynonenal (4-HNE) (ab46545, 1:200 dilution; Abcam, USA), P-Tau (ab109390, 1:4000 dilution; Abcam, USA), and Aβ1-42 (ab 12267, 1:500; Abcam) at 4 °C for 12 h, and then exposed to the secondary antibody (sc-3836, rabbit species, Santa Cruz Biotechnology, USA) for 3 h at 25 °C. The sections were photographed under a light microscope (Olympus, Japan).

Western Blotting

The seeded HT22 cells underwent the 3-h pre-incubation with OST at doses of 20 and 40 μM prior to 24-h co-incubation with L-Glu (25 mM). The treated cells and mice brains were lysed, and the concentration of protein in samples was detected. Thirty to forty micrograms of protein were separated using 12% sodium dodecyl sulfate-polyacrylamide gel electrophoresis (SDS-PAGE) and then transferred onto nitrocellulose membranes (pore size, 0.45 μm; Invitrogen, Carlsbad, CA, USA). After 4-h blocking using 5% bovine serum albumin (BSA), the membranes were exposed to Bcl-2 (ab3214), Bax (ab32503), cleaved poly (ADP-ribose) polymerase (PARP) (ab32561), Kelch-like ECH-associated protein 1 (Keap1) (ab150654), Nrf2 (ab89443), superoxide dismutase-1 (SOD-1) (ab52950), heme oxygenase-1 (HO-1) (ab68477) (diluted to 1:2000) (Abcam, Cambridge, MA, UK), and glyceraldehyde-3-phosphate dehydrogenase (GAPDH) (ABS16) (Millipore, Merck Millipore, Billerica, MA, USA) at dilution of 1:1000 for 12 h at 4 °C. And then, the membranes were exposed to horseradish peroxidase (HRP)-conjugated secondary antibody (E-AB-1001 and E-AB-1003) (Elabscience Biotechnology Co., Ltd., Wuhan, China) at dilution of 1:2000 for 3 h at 25 °C. The protein bands were visualized using a chemiluminescence kit (Merck Millipore, Billerica, MA, USA), and scanned using a BioSpectrum 600 imaging system (BioSpectrum600). ImageJ (1.46) was applied to analyze the densities of protein bands.

Statistical Analysis

All data were displayed as means ± standard deviations (S.D.). SPSS 18.0 software (IBM Corporation, Armonk, NY, USA) was applied for statistical analyses using a one-way analysis of variance, followed by multiple post hoc comparisons (Holm–Sidak test). Statistical significance was defined as a P value of < 0.05.

Results

OST Protected HT22 Cells Against L-Glu Caused Damage Related to Nrf2 Signaling

Compared with L-Glu-damaged HT22 cells, OST improved over 11.1% cell viability ($P < 0.05$) (Fig. 1a); however, OST alone shows no effects on cell proliferation (Fig. 1a). The 3-h pre-incubation of OST prior to 24-h co-incubation with L-Glu resulted in > 29.5% ($P < 0.01$) (Fig. 1b), 25.9% ($P < 0.05$) (Fig. 1c), and > 21.5% ($P < 0.05$) (Fig. 1d) reduction on the activity levels of caspase-3, caspase-8, and caspase-9 in HT22 cells.

The dissociation of MMP was noted in L-Glu-damaged HT22 cells, indicated by the reduced levels of red fluorescence and the enhanced levels of green fluorescence ($P < 0.05$) (Fig. 2a), which were strongly restored by OST incubation ($P < 0.05$) (Fig. 2a).

The 3-h pre-incubation of OST prior to 24-h co-incubation with L-Glu suppressed > 49.5% intracellular ROS levels indicated by the reduced green fluorescence intensity in HT22 cells ($P < 0.05$) (Fig. 2b).

Nrf2 played a key role in mitochondrial apoptosis via regulating the levels of its downstream proteins [5]. Compared with L-Glu damaged cells, the 3-h pre-incubation of OST prior

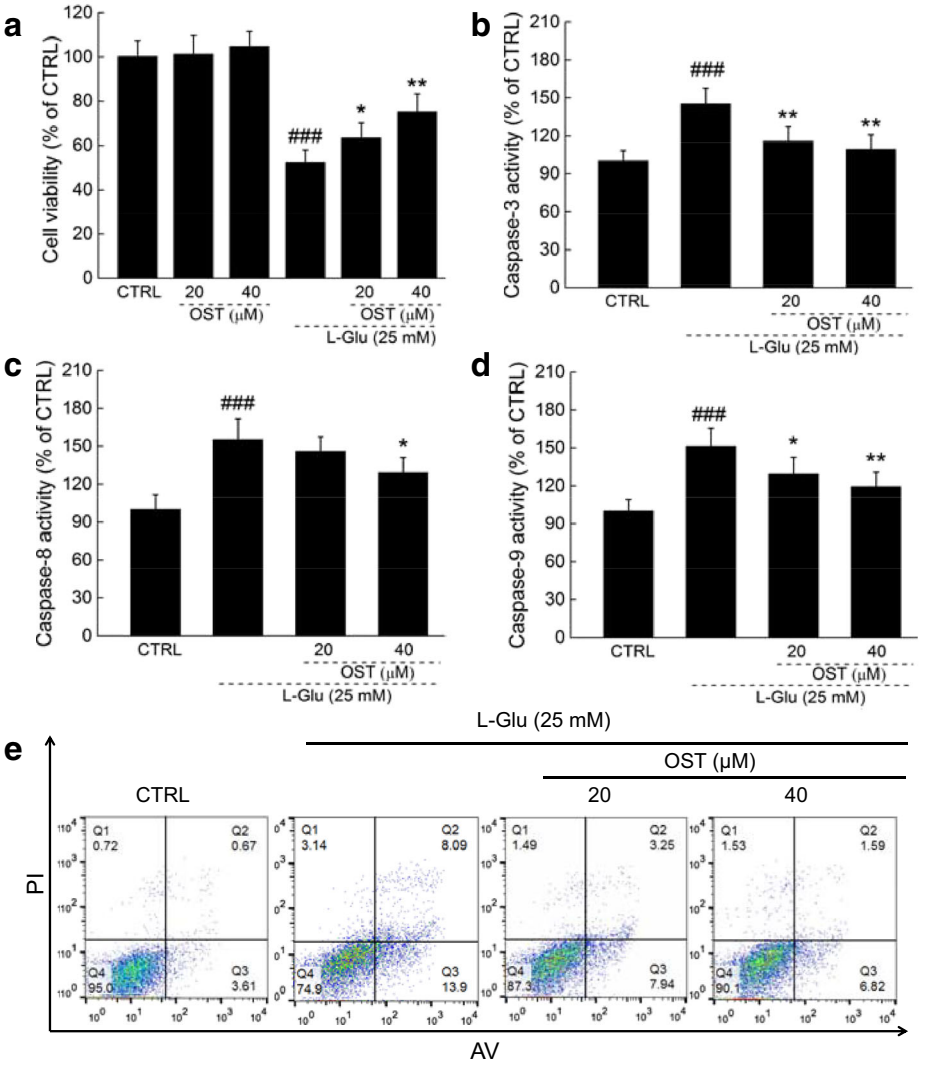

Fig. 1 The protection of OST against L-Glu-damaged HT22 cells. **a** OST enhanced the cell viability of HT22 cells exposed to L-Glu for 24 h. The 3-h pre-treatment with OST prior to the 24-h co-exposure with L-Glu **a** enhanced the cell viability, reduced the activity levels of **b** caspase 3, **c** caspase 8 and **d** caspase 9, and **e** inhibited the apoptotic rate of HT22 cells. Data are expressed as mean ± S.D. ($n = 8$). $^{###}P < 0.001$ vs. control cells, $^{*}P < 0.05$ and $^{**}P < 0.01$ vs. L-Glu-exposed cells

to 24-h co-incubation enhanced the expression levels of Bcl-2 ($P < 0.001$), Nrf2 ($P < 0.05$), HO-1 ($P < 0.001$), and SOD-1 ($P < 0.001$), and reduced the expression levels Bax ($P < 0.001$), cleaved PARP ($P < 0.001$), and Keap1 ($P < 0.001$) (Fig. 2c).

The Protection of OST Against AD-Like Symptoms in APP/PS1 Mice

OST, especially at dose of 30 mg/kg, improved the learning and memory abilities of APP/PS1 mice, suggested by its reduction on the time spent in finding the hidden platform in MWM test ($P < 0.01$, Fig. 3a), and suppressed the sojourn time in the central area in the open-field test ($P < 0.001$, Fig. 3b).

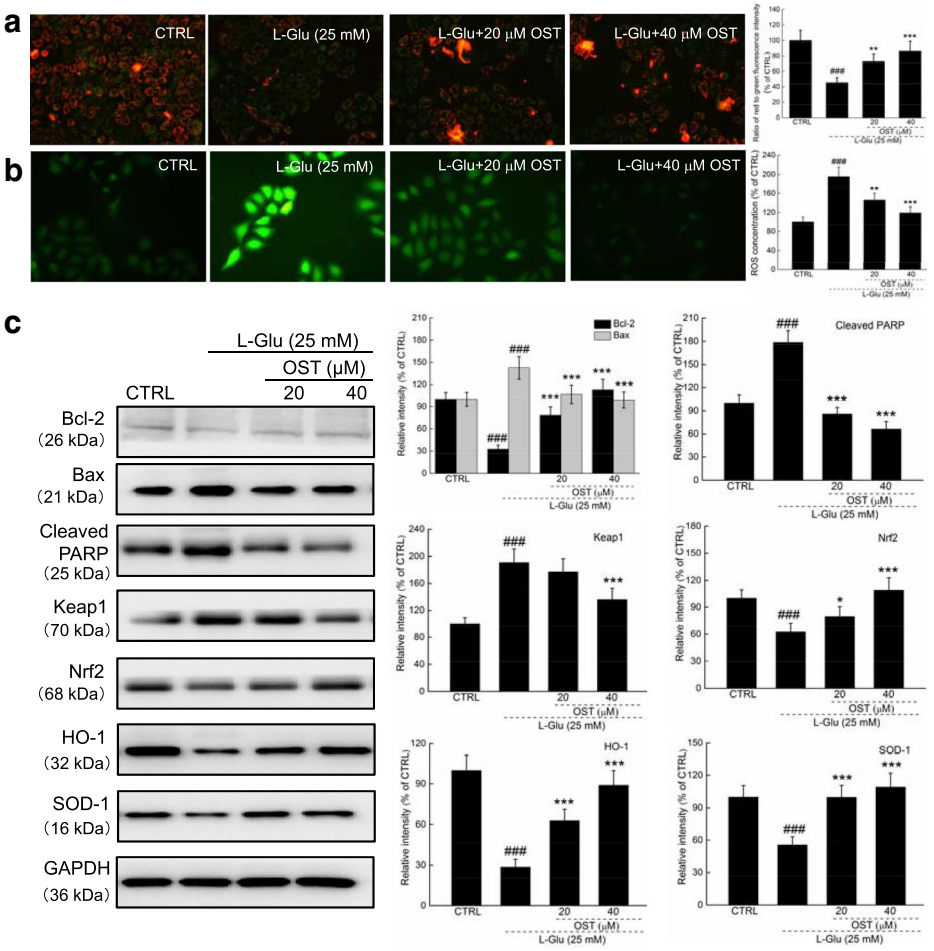

Fig. 2 The protection of OST against L-Glu causing damage in HT22 cells is partially related to its modulation on Nrf2 signaling. The HT22 cells underwent a 3-h pre-treatment with OST prior to the 24-h co-exposure with L-Glu. **a** OST restored the dissipation of MMP (× 20). **b** OST suppressed the intracellular levels of ROS. **c** OST reduced the expression levels of Bax, cleaved PARP and Keap1, and enhanced the expression levels of Bcl-2, Nrf2, SOD-1, and HO-1. The quantitative protein expression levels were normalized to that of GAPDH. Data are expressed as mean ± S.D. ($n = 8$). $^{\#\#\#}P < 0.001$ vs. control cells, $^{*}P < 0.05$, $^{**}P < 0.01$, and $^{***}P < 0.001$ vs. L-Glu exposed cells

In the brains of vehicle-treated APP/PS1 mice, the strongly enhanced numbers of Aβ1–42 (Fig. 3d) and neuronal fiber tangles due to the over-expressed P-Tau (Fig. 3c) were noted, which were suppressed by 8-week OST administration (Fig. 3c, d). Compared with vehicle-treated APP/PS1 mice, OST strongly suppressed the expression levels of 4-HNE in the brains (Fig. 3e).

The Regulation of OST on Nrf2 Signaling in APP/PS1 Mice

OST treatment resulted in the reduction on the expression levels of Keap1 ($P < 0.001$), and the enhancement on the expression levels of Nrf2 ($P < 0.05$) and its downstream proteins including HO-1 ($P < 0.001$) and SOD-1 ($P < 0.05$) (Fig. 4) in brains of APP/PS1 mice.

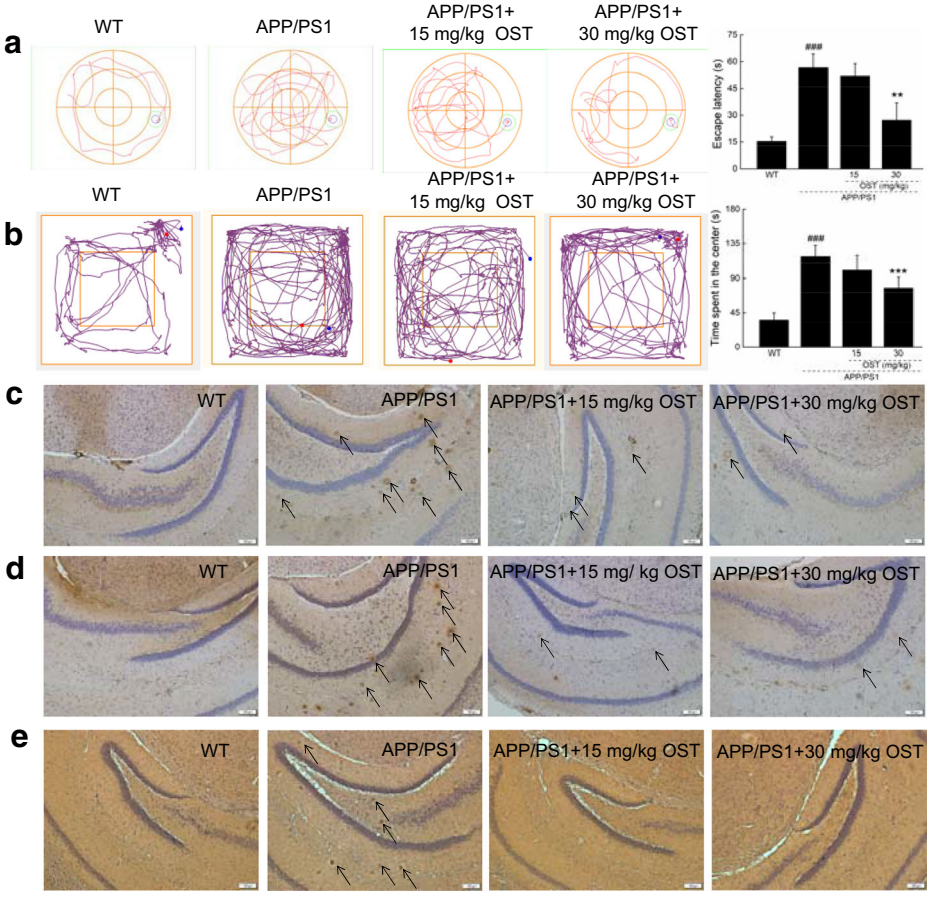

Fig. 3 The AD-like behaviors of APP/PS1 mice were strongly remitted after 8-week OST treatment. OST, especially at dose of 30 mg/kg, reduced **a** the time spent in finding the hidden platform during the MWM test and **b** the time spent in the central area of the open-field test. Data are expressed as mean ± S.D. ($n = 12$). $^{###}P < 0.001$ vs. wild-type mice, $^{**}P < 0.01$ and $^{***}P < 0.001$ vs. vehicle-treated APP/PS1 mice. In the brains of APP/PS1 mice, OST suppressed **c** the levels of P-Tau (× 100, scale bar 100 μm) ($n = 6$), **d** the deposition of Aβ1–42 (× 100, scale bar 100 μm) ($n = 6$), and **e** the expression levels of 4-HEN (× 100, scale bar 100 μm) ($n = 6$). The arrows showed the pathologic changes among experimental groups

Discussion

In the present study, it was first reported that the protection of OST against AD-like symptoms in L-Glu caused HT22 apoptotic cell model and APP/PS1 mice. As the excitatory neurotransmitter, L-Glu causes neuron damage due to its neuro-excitotoxicity and the activation of glutamate receptor causing mitochondrial fission [11]. The imbalance of expression levels of Bax and Bcl-2 is further responsible for the mitochondrial permeability leading to the activation of caspase-3 [12]. PARP is involved in DNA repair and programmed cell death [13]. OST restored the dissipation of MMP, inhibited the high expression of cleaved PARP, and reduced the levels of caspase-3, caspase-8, and caspase-9 in L-Glu-damaged HT22 cells. The activated caspase-8 caused by extracellular apoptotic stimuli [14] and the activated caspase-9 caused by cytochrome c releasing from mitochondria help to activate caspase-3 to play the key role in the execution of the apoptotic program [15]. Furthermore, during the occurrence of oxidative stress, the enhanced intracellular levels of ROS contribute to the mitochondrial depolarization [1]. According to the feedback loop, the damaged mitochondria, the primary source of ROS, releases an amount of ROS to cytoplasm [16]. Based on our present data, the protection of OST against L-Glu causing apoptosis is partially related to its modulation on mitochondrial apoptotic signaling. The overexpression of APP combining with the mutant PS1 are responsible for elevating Aβ1–42 levels [17]. APP/PS1 mice can mimic the dysfunction on learning and memory abilities which are observed in AD patients [18]. OST strongly improved the behaviors in APP/PS1 mice detected via open-field test and MWM test. The enhanced levels of Aβ deposits and neuronal fiber tangles lead the mitochondrial dysfunction to induce the over-generation of ROS, which are responsible for the damage of neurons [19, 20]. Aβ has always been regarded as an important inducer in the pathogenesis of AD [21]. Eight-week OST administration alleviated the deposition of Aβ1–42 and the hyper-expressions of phosphor-Tau in brains of APP/PS1 mice.

The broken redox equilibrium caused the oxidative stress, which has been recognized as one of the pathogeneses of AD [1]. In L-Glu-exposed HT22 cells, OST suppressed the over-

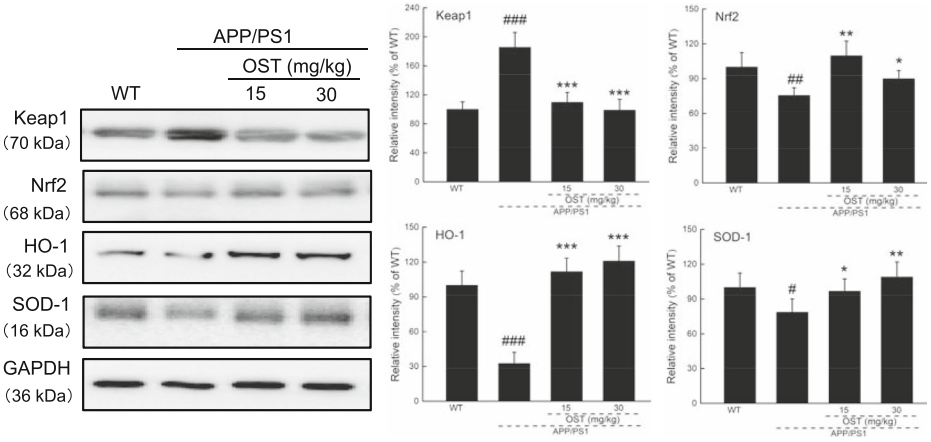

Fig. 4 OST regulated the Nrf2 signaling in brains of APP/PS1 mice. Eight-week administration of OST resulted in the reduction on the expression levels of Keap1, and the enhancements of the expression levels of Nrf2, SOD-1, and HO-1 in the whole brain lysis. The quantitative protein levels were normalized to that of GAPDH. Data are expressed as mean ± S.D. ($n = 6$). $^{\#}P < 0.05$, $^{\#\#}P < 0.01$, and $^{\#\#\#}P < 0.001$ vs. wild-type mice, $^{*}P < 0.05$, $^{**}P < 0.01$, and $^{***}P < 0.001$ vs. vehicle-treated APP/PS1 mice

accumulation of intracellular ROS levels and enhanced the expression levels of Nrf2, known as a factor regulating over 200 genes related to cellular homeostasis, which can influence the mitochondrial respiratory chain [5]. After dissociating from the complex with Keap-1, Nrf2 translocases to the nucleus and further regulates the expressions of SOD-1 and HO-1 [1, 5]. As the important antioxidant defense factors, SOD-1 and HO-1 directly deactivate the toxicity of superoxide radicals, which are considered the cascade protection from Nrf2 signaling [22, 23]. In brains of APP/PS1 mice, OST suppressed the expression levels of HNE, which is responsible for cell death due to the activation of caspases and disrupting glutamate transport [24]. Within the process of AD, the over-production of ROS is responsible for the dysfunction of mitochondrial respiration in neurons and astrocytes [25], the aggregation of Aβ1–42 [26] and the formation of neurofibrillary tangles due to the initiation of Tau [27]. OST improved the AD-like symptoms, which is at least partially related to the modulation on Nrf2 signaling to improve the defense systems against oxidative stress.

There are still limitations in the present study. We only focus the effects of OST on the neuron apoptosis, the deposition of Aβ1–42, and the neuronal fiber tangles formed by over-expressed P-Tau; however, the effects of OST on acetyl cholinergic system are not detected. Moreover, the safety use of OST should be further investigated via chronic toxicity test.

In conclusion, via applying L-Glu exposed HT22 cells and APP/PS1 mice, we first found the neuroprotection of OST against AD-like symptoms. Our data also suggested that the protective effects of OST are mainly related to its modulation on oxidative stress, especially Nrf2 signaling. Our experiment provides the evidences for further investigating the possibility of OST as a candidate for AD adjuvant therapy.

Funding Information This work was supported by the Medical Health Project in Jilin Province of P. R. China (Grant No.20191102027YY), "Thirteenth Five-Year" Science and Technology Planning Project of Jilin Province in P. R. China (Grant No. JJKH20190060KJ), and the Science Foundation of Jilin Province in P. R. China (Grant No. 20180101098JC).

Compliance with Ethical Standards

Conflict of Interest The authors declare that there is no conflict of interest.

Ethical Approval The experimental animal protocol was approved by the Animal Ethics Committee of the Second Hospital of Jilin University (20171201).

References

1. Cheignon, C., Tomas, M., Bonnefont-Rousselot, D., Faller, P., Hureau, C., & Collin, F. (2018). Oxidative stress and the amyloid beta peptide in Alzheimer's disease. *Redox Biology, 14*, 450–464.
2. de Oliveira, R. B., Gravina, F. S., Lim, R., Brichta, A. M., Callister, R. J., & van Helden, D. F. (2012). Heterogeneous responses to antioxidants in noradrenergic neurons of the locus coeruleus indicate differing susceptibility to free radical content. *Oxidative Medicine and Cellular Longevity, 2012*, 820285.
3. Rosello, A., Warnes, G., & Meier, U. C. (2012). Cell death pathways and autophagy in the central nervous system and its involvement in neurodegeneration, immunity and central nervous system infection: to die or not to die–that is the question. *Clinical and Experimental Immunology, 168*(1), 52–57.
4. Kim, D. H., Kim, D. W., Jung, B. H., Lee, J. H., Lee, H., Hwang, G. S., Kang, K. S., & Lee, J. W. (2019). Ginsenoside Rb2 suppresses the glutamate-mediated oxidative stress and neuronal cell death in HT22 cells. *Journal of Ginseng Research, 43*(2), 326–334.

5. Joshi, G., Gan, K. A., Johnson, D. A., & Johnson, J. A. (2015). Increased Alzheimer's disease-like pathology in the APP/ PS1DeltaE9 mouse model lacking Nrf2 through modulation of autophagy. *Neurobiology of Aging, 36*(2), 664–679.
6. Deshpande, P., Gogia, N., & Singh, A. (2019). Exploring the efficacy of natural products in alleviating Alzheimer's disease. *Neural Regeneration Research, 14*(8), 1321–1329.
7. Bi, D. B., Yang, M. S., Zhao, X., & Huang, S. M. (2015). Effect of Cnidium lactone on serum mutant P53 and BCL-2/BAX expression in human prostate cancer cells PC-3 tumor-bearing BALB/C nude mouse model. *Medical Science Monitor, 21*, 2421–2427.
8. Fan, H., Gao, Z., Ji, K., Li, X., Wu, J., Liu, Y., Wang, X., Liang, H., Liu, Y., Li, X., Liu, P., Chen, D., & Zhao, F. (2019). The in vitro and in vivo anti-inflammatory effect of osthole, the major natural coumarin from Cnidium monnieri (L.) Cuss, via the blocking of the activation of the NF-kappaB and MAPK/p38 pathways. *Phytomedicine: International Journal of Phytotherapy and Phytopharmacology, 58*, 152864.
9. Li, Z., Chen, X., Lu, W., Zhang, S., Guan, X., Li, Z., & Wang, D. (2017). Anti-oxidative stress activity is essential for Amanita caesarea mediated neuroprotection on glutamate-induced apoptotic HT22 cells and an Alzheimer's disease mouse model. *International Journal of Molecular Sciences, 18*(8).
10. An, S., Lu, W., Zhang, Y., Yuan, Q., & Wang, D. (2017). Pharmacological basis for use of Armillaria mellea polysaccharides in Alzheimer's disease: antiapoptosis and antioxidation. *Oxidative Medicine and Cellular Longevity, 2017*, 4184562.
11. Liot, G., Bossy, B., Lubitz, S., Kushnareva, Y., Sejbuk, N., & Bossy-Wetzel, E. (2009). Complex II inhibition by 3-NP causes mitochondrial fragmentation and neuronal cell death via an NMDA- and ROS-dependent pathway. *Cell Death and Differentiation, 16*(6), 899–909.
12. Bivik, C. A., Larsson, P. K., Kagedal, K. M., Rosdahl, I. K., & Ollinger, K. M. (2006). UVA/B-induced apoptosis in human melanocytes involves translocation of cathepsins and Bcl-2 family members. *The Journal of Investigative Dermatology, 126*(5), 1119–1127.
13. Piskunova TS, Yurova MN, Ovsyannikov AI, Semenchenko AV, Zabezhinski MA, Popovich IG, Wang ZQ, Anisimov VN (2008) Deficiency in poly(ADP-ribose) polymerase-1 (PARP-1) accelerates aging and spontaneous carcinogenesis in mice. Current Gerontology and Geriatrics Research 754190
14. McKee, A. E., & Thiele, C. J. (2006). Targeting caspase 8 to reduce the formation of metastases in neuroblastoma. *Expert Opinion on Therapeutic Targets, 10*(5), 703–708.
15. Li, P., Zhou, L., Zhao, T., Liu, X., Zhang, P., Liu, Y., Zheng, X., & Li, Q. (2017). Caspase-9: structure, mechanisms and clinical application. *Oncotarget, 8*(14), 23996–24008.
16. Tang, X.-Q., Feng, J.-Q., Chen, J., Chen, P.-X., Zhi, J.-L., Cui, Y., Guo, R.-X., & Yu, H.-M. (2005). Protection of oxidative preconditioning against apoptosis induced by H2O2 in PC12 cells: mechanisms via MMP, ROS, and Bcl-2. *Brain Research, 1057*(1–2), 57–64.
17. Bilkei-Gorzo, A. (2014). Genetic mouse models of brain ageing and Alzheimer's disease. *Pharmacology & Therapeutics, 142*(2), 244–257.
18. Varadarajan, S., Yatin, S., Aksenova, M., & Butterfield, D. A. (2000). Review: Alzheimer's amyloid beta-peptide-associated free radical oxidative stress and neurotoxicity. *Journal of Structural Biology, 130*(2–3), 184–208.
19. Calderon-Garciduenas, A. L., & Duyckaerts, C. (2017). Alzheimer disease. *Handbook of Clinical Neurology, 145*, 325–337.
20. Kim, D. I., Lee, K. H., Gabr, A. A., Choi, G. E., Kim, J. S., Ko, S. H., & Han, H. J. (2016). A beta-induced Drp1 phosphorylation through Akt activation promotes excessive mitochondrial fission leading to neuronal apoptosis. *Biochimica et Biophysica Acta, 1863*(11), 2820–2834.
21. Santana, I., Baldeiras, I., Santiago, B., Duro, D., Freitas, S., Pereira, M. T., Almeida, M. R., & Oliveira, C. R. (2018). Underlying biological processes in mild cognitive impairment: amyloidosis versus neurodegeneration. *Journal of Alzheimer's Disease, 64*(s1), S647–SS57.
22. Kaur, S. J., McKeown, S. R., & Rashid, S. (2016). Mutant SOD1 mediated pathogenesis of amyotrophic lateral sclerosis. *Gene, 577*(2), 109–118.
23. Hettiarachchi, N., Dallas, M., Al-Owais, M., Griffiths, H., Hooper, N., Scragg, J., Boyle, J., & Peers, C. (2014). Heme oxygenase-1 protects against Alzheimer's amyloid-beta(1-42)-induced toxicity via carbon monoxide production. *Cell Death & Disease, 5*(12), e1569.
24. Butterfield, D. A., Castegna, A., Lauderback, C. M., & Drake, J. (2002). Evidence that amyloid beta-peptide-induced lipid peroxidation and its sequelae in Alzheimer's disease brain contribute to neuronal death. *Neurobiology of Aging, 23*(5), 655–664.
25. Fossati, S., Giannoni, P., Solesio, M. E., Cocklin, S. L., Cabrera, E., Ghiso, J., & Rostagno, A. (2016). The carbonic anhydrase inhibitor methazolamide prevents amyloid beta-induced mitochondrial dysfunction and caspase activation protecting neuronal and glial cells in vitro and in the mouse brain. *Neurobiology of Disease, 86*, 29–40.

26. Spilovska, K., Korabecny, J., Nepovimova, E., Dolezal, R., Mezeiova, E., Soukup, O., & Kuca, K. (2017). Multitarget tacrine hybrids with neuroprotective properties to confront Alzheimer's disease. *Current Topics in Medicinal Chemistry, 17*(9), 1006–1026.
27. Zhao, J. M., Li, L., Chen, L., Shi, Y., Li, Y. W., Shang, H. X., Wu, L. Y., Weng, Z. J., Bao, C. H., & Wu, H. G. (2017). Comparison of the analgesic effects between electro-acupuncture and moxibustion with visceral hypersensitivity rats in irritable bowel syndrome. *World Journal of Gastroenterology, 23*(16), 2928–2939.

Affiliations

Qiubo Chu[1,2] · Yanfeng Zhu[2] · Tianjiao Cao[2] · Yi Zhang[2] · Zecheng Chang[3] · Yan Liu[2] · Jiahui Lu[2] · Yizhi Zhang[1]

Qiubo Chu
chuqb17@mails.jlu.edu.cn

Yanfeng Zhu
zhuyf1317@mails.jlu.edu.cn

Tianjiao Cao
caotj9917@mails.jlu.edu.cn

Yi Zhang
zhangyi1315@mails.jlu.edu.cn

Zecheng Chang
changzc2716@mails.jlu.edu.cn

Yan Liu
liuyan7511@jlu.edu.cn

Jiahui Lu
lujh@jlu.edu.cn

[1] Department of Neurology, the Second Hospital of Jilin University, Jilin University, Changchun 130041, China

[2] School of Life Sciences, Jilin University, Changchun 130012, China

[3] School of Public Health, Jilin University, Changchun 130012 Jilin, China